Journal of Sound and Vibration (1997) **199**(3), 431–452

SHELL–PLATE INTERACTION IN THE FREE VIBRATIONS OF CIRCULAR CYLINDRICAL TANKS PARTIALLY FILLED WITH A LIQUID: THE ARTIFICIAL SPRING METHOD

M. Amabili

Dipartimento di Meccanica, Università di Ancona, I-60131 Ancona, Italy

(*Received* 19 *October* 1995, *and in final form* 27 *June* 1996)

The free vibrations of a circular cylindrical tank partially filled with an inviscid and incompressible liquid with a free surface orthogonal to the tank axis are analytically studied. The tank is modelled by a simply supported circular cylindrical shell connected to a simply supported circular plate by an artificial rotational distributed spring of appropriate stiffness. The plate is considered to be resting on a Winkler elastic foundation. The effects of the free surface waves and the hydrostatic liquid pressure are neglected. The bulging modes (where the tank walls oscillate with the liquid) of the structure are investigated and the solution is obtained as an eigenvalue problem by using the Rayleigh–Ritz expansion of the mode shapes and then minimizing the Rayleigh quotient for coupled vibrations. The effects of the liquid level inside the tank, of the stiffness of the Winkler foundation and of the spring stiffness at the shell–plate joint are investigated for shallow and tall water-filled tanks. Comparison with available results is also given.

1. INTRODUCTION

During recent years, many papers on the vibrations of structures made by joining simple elements together have been published. Different techniques have been used, such as the artificial spring method [1–4], the transfer matrix method [5] and the receptance method [6–8]. Recently, these techniques have been applied by some authors to cylindrical shell–circular plate structures [2, 4–9]. Different approaches to similar problems have given an incentive for research in this field.

The Rayleigh–Ritz method has been proved to be very efficient in studying complex structures but, in order to obtain correct results, the trial functions must satisfy all the geometrical boundary conditions. When the Rayleigh–Ritz method is applied to a structure obtained by joining some components together, the boundary conditions require the continuity of translational and rotational displacements between all the rigid junctions of the substructures. This condition causes many problems in the choice of the correct trial functions to use for each single component. The use of artificial springs at the junctions allows one to overcome this difficulty. In particular, the joints between the components of the structure are represented by translational and rotational artificial springs that are distributed along the whole joint length or area. Obviously, each degree of freedom involved in the joint must be simulated by a distributed spring.

The plate-ended circular cylindrical shell is the simpler plate–shell structure and it is also important for application to engineering. Free vibrations of this structure have been studied, e.g., by Cheng and Nicolas [2] and by Huang and Soedel [6]. Cheng [9] has also

0022–460X/97/030431 + 22 $25.00/0/sv960650

studied the free vibrations when the plate-ended circular cylindrical shell is coupled with a fluid-filled acoustic cavity. A common application of this structure is the tank; tanks are often coupled with a liquid having a free surface. The liquid-filled tanks have two families of modes: sloshing and bulging. Sloshing modes are caused by the oscillation of the liquid free surface, due to the rigid body movement of the container; these modes are also affected by the flexibility of the container. The vibrations of the tank walls (bottom plate and shell) take the name of bulging modes when the amplitude of the wall displacement is dominant over that of the free surface; in this case, the tank walls and base oscillate with the liquid. The velocity field of the liquid in a circular cylindrical tank has been studied by Bauer and Siekmann [10]. However, they considered the shell and the plate to be independent and not coupled together; moreover, they were interested in sloshing modes.

The present paper reports a study of a tank partially filled with an inviscid and incompressible liquid having a free surface orthogonal to the tank axis. The tank is modelled by a simply supported circular cylindrical shell connected to a simply supported circular plate by an artificial rotational distributed spring of opportune stiffness. The plate is considered to be resting on a Winkler elastic foundation. This model is quite realistic because the connection between the plate and the shell gives a reciprocal constraint that can be assumed to be a simple support. In many applications, the top of the tank is closed by a thin diaphragm or by a ring that constrains the shell displacements in a manner similar to that of a simple support (except for beam-bending modes). Moreover, the effect of the soil stiffness can also be modelled by the Winkler elastic foundation. The bulging modes of the structure are investigated and the solution is obtained as an eigenvalue problem by using the Rayleigh–Ritz method.

2. THEORETICAL APPROACH TO THE SHELL–PLATE STRUCTURE

A simply supported circular cylindrical shell made of isotropic, homogeneous and linearly elastic material is considered, so that the Flügge theory of shells [11] is applicable. A simply supported thin circular plate is connected to a shell end and rests on a Winkler elastic foundation [12]; it is also assumed that the plate is made of isotropic, homogeneous and linearly elastic material, so that the Kirchhoff theory of plate vibrations [13] is applicable.

When a plate is joined to a circular cylindrical shell, in general three displacements and two slope connections should be considered, according to the classical thin shell theory. However, the full treatment of using five connections is not necessary if one investigates only lower modes of the system. For these modes, the plate can be assumed to be inelastic in its plane and to allow only transverse displacements. Moreover, influences of connection deflections in the tangential planes of the shell can be neglected with respect to transverse amplitudes [6]. Therefore only the radial slope at the plate boundary can be considered to be coupled to the axial slope of the shell at the bottom end. A similar approach was used in reference [14]; in references [6–8] two connections were used because the plate was not connected to the shell's simple support. In the present case, only one connection is required; the shell and the plate are connected together by an artificial rotational distributed spring of opportune stiffness (Figure 1) in order to obtain a tank of radius a and height L.

A cylindrical polar co-ordinate system $(O; r, \theta, x)$ is introduced, with the pole on the centre of the circular bottom plate. Due to the axial symmetry of the structure, only modes of the shell and the plate with the same number n of nodal diameters are coupled. In particular, in the present study both the axisymmetric vibrations ($n = 0$) and asymmetric vibrations ($n > 0$) are investigated. In addition, it is interesting to note that, due to the

axial symmetry, for each asymmetric mode there exists a second mode having the same frequency and shape but angularly rotated by $\pi/2n$.

The Rayleigh–Ritz method [15] is applied to find the mode shapes of the circular cylindrical tank. Therefore, the radial displacement w of the shell wall (see Figure 1) can be given by the expression

$$w(x, \theta) = \cos(n\theta) \sum_{s=1}^{\infty} q_s B_s \sin(s\pi x/L), \tag{1}$$

where n is the number of nodal diameters, q_s are the unknown parameters and B_s is a constant depending on the normalization criterion used. The eigenvectors of the single and empty simply supported shell [11] are used as admissible functions. Then the following normalization is introduced

$$(L/a)^2 \int_0^1 B_s^2 \sin^2(s\pi l)\, \mathrm{d}l = 1, \tag{2}$$

where $l = x/L$. The result of the integration gives

$$B_s = B = \sqrt{2}\, a/L \tag{3}$$

The transverse displacement, w_P, of the plate can be given as [16]

$$w_P(r, \theta) = \cos(n\theta) \sum_{i=0}^{\infty} \tilde{q}_i \left[A_{in} \mathrm{J}_n\left(\frac{\lambda_{in} r}{a}\right) + C_{in} \mathrm{I}_n\left(\frac{\lambda_{in} r}{a}\right) \right], \tag{4}$$

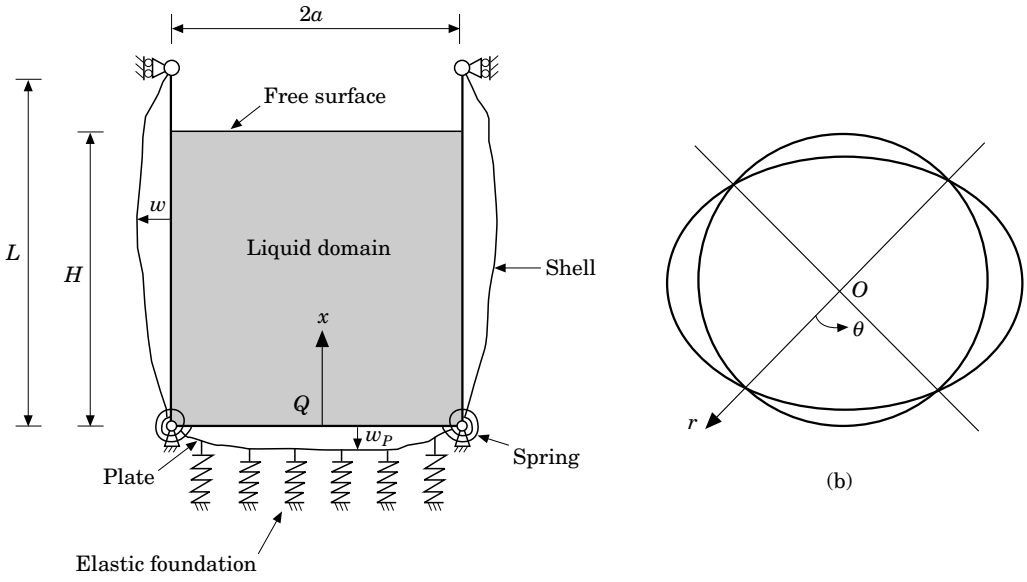

Figure 1. A diagram of the tank and of the symbols used: (a) the cross-section defined by $\theta = 0$ and $\theta = \pi$; (b) the mode shape with $n = 2$ nodal diameters in the cross-section defined by $x = L/2$.

where n and i are the number of nodal diameters and circles, respectively, a is the plate radius and λ_{in} is the well known frequency parameter that is related to the plate natural frequency; J_i and I_i are the Bessel function and modified Bessel function of order i, respectively. In equation (4), the eigenfunctions of the single plate, simply supported at the edge and vibrating in a vacuum, are assumed as admissible functions. The trial functions are linearly independent and constitute a complete set. Values of λ_{in} for simply supported plates are given, for example, in reference [17]. To simplify the computations, the mode shape constants, A_{in} and C_{in}, are normalized in order to have

$$\int_0^1 [A_{in}\mathrm{J}_n(\lambda_{in}\rho) + C_{in}\mathrm{I}_n(\lambda_{in}\rho)]^2\rho \, \mathrm{d}\rho = 1, \tag{5}$$

where $\rho = r/a$. The result of integration of equation (5) is (see equations 11.106, 33.101 and 31.101 in reference [18])

$$\left\{\frac{A_{in}^2}{2}\left[(\mathrm{J}_n'(\lambda_{in}))^2 + \left(1 - \frac{n^2}{\lambda_{in}^2}\right)\mathrm{J}_n^2(\lambda_{in})\right] - \frac{C_{in}^2}{2}\left[(\mathrm{I}_n'(\lambda_{in}))^2 - \left(1 + \frac{n^2}{\lambda_{in}^2}\right)\mathrm{I}_n^2(\lambda_{in})\right]\right.$$

$$\left. + \frac{A_{in}C_{in}}{\lambda_{in}}[\mathrm{J}_n(\lambda_{in})\mathrm{I}_{n+1}(\lambda_{in}) + \mathrm{I}_n(\lambda_{in})\mathrm{J}_{n+1}(\lambda_{in})]\right\} = 1, \tag{6}$$

where J_n' and I_n' indicate the derivatives of J_n and I_n with respect to the argument. The ratio of the mode shape constants $A_{in}/C_{in} = -\mathrm{I}_n(\lambda_{in})/\mathrm{J}_n(\lambda_{in})$ for simply supported plates.

In order to solve the problem, one evaluates the kinetic and potential energies of the shell, plate, liquid, elastic foundation and coupling spring. The reference kinetic energy [15] of the shell, neglecting the tangential inertia, is given by

$$T_S^* = \tfrac{1}{2}\rho_S h_S B^2 \int_0^{2\pi}\int_0^L w^2 \, \mathrm{d}x \, a \, \mathrm{d}\theta = \tfrac{1}{2}\rho_S a h_S \frac{L}{2} B^2 \psi_n \sum_{s=1}^{\infty} q_s^2, \tag{7}$$

where h_S is the shell thickness, ρ_S is the density of the shell material (kg m^{-3}) and

$$\psi_n = \begin{Bmatrix} 2\pi, & \text{for } n = 0 \\ \pi, & \text{for } n > 0 \end{Bmatrix}.$$

In equation (7) the orthogonality of the sine function is used. Similarly, the reference kinetic energy of the plate is given by

$$T_P^* = \tfrac{1}{2}\rho_P h_P \int_0^{2\pi}\int_0^a w_P^2 r \, \mathrm{d}r \, \mathrm{d}\theta = \tfrac{1}{2}\rho_P a^2 h_P \psi_n \sum_{i=0}^{\infty} \tilde{q}_i^2, \tag{8}$$

where h_P is the plate thickness and ρ_P is the density of the plate material (kg m^{-3}). In equation (8) the orthogonality of the Bessel functions (plate mode shapes) is used. Then, the maximum potential energy of each mode of the single and empty shell is equal to the product of the reference kinetic energy of the same mode for the square circular frequency ω_s^2 of this mode. Moreover, in coupled vibrations, due to the series expansion of the mode shape, the potential energy is the sum of the energies of each single component mode.

Therefore the maximum potential energy of the shell is given by

$$V_S = \tfrac{1}{2}\rho_S h_S a \frac{L}{2} B^2 \psi_n \sum_{s=1}^{\infty} q_s^2 \omega_s^2, \tag{9}$$

where ω_s are the circular frequencies of the flexural modes of the simply supported shell that can be computed by using the Flügge theory of shells [11]. Similarly, the maximum potential energy of the plate is the sum of the reference kinetic energies of the eigenfunctions of the plate in a vacuum multiplied by $\tilde{\omega}_{in}^2$,

$$V_P = \tfrac{1}{2}\rho_P a^2 h_P \psi_n \sum_{i=0}^{\infty} \tilde{q}_i^2 \tilde{\omega}_{in}^2 = \tfrac{1}{2}\frac{D}{a^2}\psi_n \sum_{i=0}^{\infty} \tilde{q}_i^2 \lambda_{in}^4, \tag{10}$$

where the plate circular frequency $\tilde{\omega}_{in}$ is related to the frequency parameter λ_{in} by $\tilde{\omega}_{in} = (\lambda_{in}^2/a^2)\sqrt{D/(\rho_P h_P)}$ and $D = E_P h_P^3/[12(1-\nu_P^2)]$ is the flexural rigidity of the plate; ν_P and E_P are the Poisson ratio and Young's modulus of the plate, respectively. The maximum potential energy of the rotational distributed spring connecting the plate and the shell is

$$V_C = \tfrac{1}{2}\int_0^{2\pi} c_1[(\partial w/\partial x)_{x=0} - (\partial w_P/\partial r)_{r=a}]^2 a \, \mathrm{d}\theta, \tag{11}$$

where c_1 is the spring stiffness (Nm/m). It is interesting to note that the sign to rotations is attributed by considering that both w and w_P are assumed to be positive outside the tank (see Figure 1), so that both the displacements give a positive contribution to the increment of the angle between the shell and the plate, which gives a compression to the rotational spring. The rotation of the shell end at $x = 0$ is given by

$$\left(\frac{\partial w}{\partial x}\right)_{x=0} = \frac{B\pi}{L}\cos(n\theta)\sum_{s=1}^{\infty} q_s s. \tag{12}$$

The rotation of the plate edge, changed by sign, is

$$\left(\frac{\partial w_P}{\partial r}\right)_{r=a} = \cos(n\theta)\sum_{i=0}^{\infty}\tilde{q}_i\frac{\lambda_{in}}{a}[A_{in}\mathrm{J}_n'(\lambda_{in}) + C_{in}\mathrm{I}_n'(\lambda_{in})]. \tag{13}$$

Therefore, by using equations (11)–(13), the maximum potential energy stored by the coupling spring is given by the expression

$$V_C = \tfrac{1}{2}c_1\Bigg\{B^2\frac{\pi^2}{L^2}\sum_{s=1}^{\infty}\sum_{j=1}^{\infty} q_s q_j s j + \sum_{i=0}^{\infty}\sum_{h=0}^{\infty}\tilde{q}_i\tilde{q}_h\frac{\lambda_{in}}{a}\frac{\lambda_{hn}}{a}[A_{in}\mathrm{J}_n'(\lambda_{in}) + C_{in}\mathrm{I}_n'(\lambda_{in})]$$

$$\times [A_{hn}\mathrm{J}_n'(\lambda_{hn}) + C_{hn}\mathrm{I}_n'(\lambda_{hn}) - 2B\frac{\pi}{L}\sum_{s=1}^{\infty}\sum_{i=0}^{\infty} q_s\tilde{q}_i s\frac{\lambda_{in}}{a}[A_{in}\mathrm{J}_n'(\lambda_{in}) + C_{in}\mathrm{I}_n'(\lambda_{in})]\Bigg\}a\psi_n. \tag{14}$$

The maximum potential energy stored by the Winkler elastic foundation is

$$V_B = \tfrac{1}{2}k_1 \int_0^{2\pi} \int_0^a w_P^2 \, r \, \mathrm{d}r \, \mathrm{d}\theta = \tfrac{1}{2}k_1 \psi_n a^2 \sum_{i=0}^{\infty} \tilde{q}_i^2, \tag{15}$$

where k_1 is the stiffness of the foundation (N m^{-3}).

3. LIQUID–STRUCTURE INTERACTION

The tank is considered partially filled with an inviscid and incompressible liquid, with a free surface orthogonal to the tank axis; the free surface is at distance H from the bottom plate (see Figure 1). The free surface waves, superficial tension of the liquid and hydrostatic pressure effects are neglected in the present study [19], so that only a kinetic energy can be attributed to the liquid; therefore the sloshing modes of the tank are not obtained by the present approach and only the bulging modes are investigated. As a consequence of these hypotheses, the free surface does not exhibit an intrinsic capability of oscillation; thus the free liquid surface is not subjected to a restoring force once moved.

3.1. KINETIC ENERGY OF THE LIQUID

For an incompressible and inviscid liquid, the velocity potential satisfies the Laplace equation $\nabla^2\phi(r, \theta, x) = 0$. In the case studied, the liquid velocity potential, using the principle of superposition, is described by the sum $\phi = \phi^{(1)} + \phi^{(2)}$, where the function $\phi^{(1)}$ describes the liquid velocity potential of the flexible shell considering the bottom plate as rigid and the function $\phi^{(2)}$ describes the liquid velocity potential of the flexible bottom plate considering the shell as rigid. Therefore, by using Green's theorem for harmonic functions [20], the reference kinetic energy of the liquid can be computed by integration over the liquid boundary,

$$T_L^* = \tfrac{1}{2}\rho_L \int_S (\phi^{(1)} + \phi^{(2)}) \frac{\partial(\phi^{(1)} + \phi^{(2)})}{\partial z} \, \mathrm{d}S, \tag{16}$$

where ρ_L is the liquid mass density (kg m^{-3}), z is the direction normal at any point to the surface S and is oriented outward, $S = S_1 + S_2$, S_1 is the shell lateral surface and S_2 is the plate surface. Integration over the free liquid surface is not necessary; in fact, the liquid boundary conditions are

$$(\partial\phi^{(1)}/\partial r)_{r=a} = w(x, \theta), \qquad (\partial\phi^{(1)}/\partial x)_{x=0} = 0, \qquad (\phi^{(1)})_{x=H} = 0, \tag{17a–c}$$

and

$$(\partial\phi^{(2)}/\partial x)_{x=0} = -w_P(r, \theta), \qquad (\partial\phi^{(2)}/\partial r)_{r=a} = 0, \qquad (\phi^{(2)})_{x=H} = 0, \tag{18a–c}$$

so that the result of the extension of equation (16) on the free surface is zero. The zero dynamic pressure on the free surface is assumed as a boundary condition as a consequence of the assumed hypothesis of neglecting the free surface waves. The result of integration of equation (16) can be divided into four different terms by using equations (17a) and (18a):

$$\begin{aligned} T_L^* &= \tfrac{1}{2}\rho_L \int_{S_1} (\phi^{(1)} + \phi^{(2)}) w \, \mathrm{d}S + \tfrac{1}{2}\rho_L \int_{S_2} (\phi^{(1)} + \phi^{(2)}) w_P \, \mathrm{d}S \\ &= T_L^{*(1)} + T_L^{*(1-2)} + T_L^{*(2-1)} + T_L^{*(2)}. \end{aligned} \tag{19}$$

3.2. LIQUID–SHELL INTERACTION

In this section, the vibration problem of a simply supported flexible shell in a circular cylindrical tank with a rigid base is considered. A large number of papers on the vibrations of fluid-filled shells have been published; it is worth remembering, for example, references [21–27]. The liquid velocity potential $\phi^{(1)}$ is assumed to be of the form

$$\phi^{(1)} = \sum_{s=1}^{\infty} q_s \Phi_s^{(1)}. \tag{20}$$

The functions $\Phi_s^{(1)}$ are given by

$$\Phi_s^{(1)}(x, r, \theta) = \sum_{m=1}^{\infty} A_{mns} \mathrm{I}_n\left(\frac{2m-1}{2}\pi\frac{r}{H}\right)\cos(n\theta)\cos\left(\frac{2m-1}{2}\pi\frac{x}{H}\right), \tag{21}$$

where A_{mns} are coefficients depending on the integers m, n and s. The functions $\Phi_s^{(1)}$ satisfy the Laplace equation and the two boundary conditions given in equations (17b, c); the condition given in equation (17a) is used to compute the coefficients A_{mns}:

$$\sum_{m=1}^{\infty} A_{mns}\frac{(2m-1)\pi}{2H}\mathrm{I}_n'\left(\frac{2m-1}{2}\pi\frac{a}{H}\right)\cos(n\theta)\cos\left(\frac{2m-1}{2}\pi\frac{x}{H}\right) = B\sin\left(s\pi\frac{x}{L}\right). \tag{22}$$

If one multiplies equation (22) by

$$\cos\left(\frac{2j-1}{2}\pi\frac{x}{H}\right)$$

and then integrates between 0 and H, using the well known properties of the orthogonal functions, one obtains

$$\Phi_s^{(1)} = \sum_{m=1}^{\infty}\frac{4B}{(2m-1)\pi}\sigma_{ms}\left[\mathrm{I}_n\left(\frac{2m-1}{2}\pi\frac{r}{H}\right)\Big/\mathrm{I}_n'\left(\frac{2m-1}{2}\pi\frac{a}{H}\right)\right] \times\cos(n\theta)\cos\left(\frac{2m-1}{2}\pi\frac{x}{H}\right), \tag{23}$$

where

$$\sigma_{ms} = \left[\frac{s}{L} + (-1)^m\frac{2m-1}{2H}\sin\left(s\pi\frac{H}{L}\right)\right]\Big/\left(\frac{s^2}{L^2} - \frac{4m^2-4m+1}{4H^2}\right)\pi \qquad \text{if } s \neq \frac{2m-1}{2}\frac{L}{H}, \tag{24a}$$

or

$$\sigma_{ms} = \frac{L}{2s\pi} \qquad \text{if } s = \frac{2m-1}{2}\frac{L}{H}. \tag{24b}$$

Therefore, the term $T_L^{*(1)}$ of the reference kinetic energy of the liquid is given by

$$T_L^{*(1)} = \tfrac{1}{2}\rho_L \int_0^{2\pi}\int_0^{H} (\phi^{(1)})_{r=a} wa \, \mathrm{d}\theta \, \mathrm{d}x$$

$$= \tfrac{1}{2}\rho_L B^2 a \psi_n \sum_{s=1}^{\infty}\sum_{j=1}^{\infty} q_s q_j \sum_{m=1}^{\infty} \times \frac{4\sigma_{ms}\sigma_{jm}}{(2m-1)\pi} \frac{\mathrm{I}_n\left(\dfrac{2m-1}{2}\pi\dfrac{a}{H}\right)}{\mathrm{I}_n'\left(\dfrac{2m-1}{2}\pi\dfrac{a}{H}\right)}. \quad (25)$$

3.3. LIQUID–PLATE INTERACTION

In this section, the vibration problem of the simply supported flexible bottom plate is studied with the circular cylindrical shell assumed to be rigid [10, 12, 28–32]. The liquid velocity potential $\phi^{(2)}$ is assumed to be of the form

$$\phi^{(2)} = \sum_{i=0}^{\infty} \tilde{q}_i \Phi_i^{(2)}. \quad (26)$$

The functions $\Phi_i^{(2)}$, for axisymmetric modes ($m = 0$), are expressed as

$$\Phi_i^{(2)}(r, \theta, x) = K_{i00}(x - H) + \sum_{k=1}^{\infty} K_{i0k} \mathrm{J}_0\left(\varepsilon_{0k}\frac{r}{a}\right)\left[\cosh\left(\varepsilon_{0k}\frac{x}{a}\right)\right.$$

$$\left. - \sinh\left(\varepsilon_{0k}\frac{x}{a}\right)\Big/\tanh\left(\varepsilon_{0k}\frac{H}{a}\right)\right], \quad (27)$$

and, for asymmetric ($m > 0$) modes, as

$$\Phi_i^{(2)}(x, r, \theta) = \cos(n\theta) \sum_{k=0}^{\infty} K_{ink} \mathrm{J}_n\left(\varepsilon_{nk}\frac{r}{a}\right)\left[\cosh\left(\varepsilon_{nk}\frac{x}{a}\right) - \sinh\left(\varepsilon_{nk}\frac{x}{a}\right)\Big/\tanh\left(\varepsilon_{nk}\frac{H}{a}\right)\right], \quad (28)$$

where ε_{nk} are solutions of the equation

$$\mathrm{J}_n'(\varepsilon_{nk}) = 0. \quad (29)$$

The functions $\Phi_i^{(2)}$ satisfy equations (18b,c). The constants K_{ink} are calculated in order to satisfy equation (18a). For asymmetric modes,

$$\sum_{k=0}^{\infty} K_{ink} \mathrm{J}_n\left(\varepsilon_{nk}\frac{r}{a}\right) \frac{\varepsilon_{nk}}{a\tanh(\varepsilon_{nk}H/a)} = \left[A_{in}\mathrm{J}_n\left(\frac{\lambda_{in}r}{a}\right) + C_{in}I_n\left(\frac{\lambda_{in}r}{a}\right)\right]. \quad (30)$$

If one multiplies equation (30) by $(1/a^2)\mathrm{J}_n([\varepsilon_{nk}(r/a)]r$ and then integrates, this results in

$$K_{ink} = \frac{(A_{in}\beta_{ink} + C_{in}\gamma_{ink})}{\alpha_{nk}\varepsilon_{nk}} a \tanh\left(\varepsilon_{nk}\frac{H}{a}\right), \quad (31)$$

where

$$\alpha_{nk} = \tfrac{1}{2}[1 - (n/\varepsilon_{nk})^2][\mathrm{J}_n(\varepsilon_{nk})]^2, \qquad \beta_{ink} = \frac{\lambda_{in}}{\varepsilon_{nk}^2 - \lambda_{in}^2}\,\mathrm{J}'_n(\lambda_{in})\mathrm{J}_n(\varepsilon_{nk}),$$

$$\gamma_{ink} = \frac{\lambda_{in}}{\varepsilon_{nk}^2 + \lambda_{in}^2}\,\mathrm{I}'_n(\lambda_{in})\mathrm{J}_n(\varepsilon_{nk}). \tag{32–34}$$

Then, the term $T_L^{*(2)}$ of the reference kinetic energy of the liquid is given by

$$T_L^{*(2)} = \tfrac{1}{2}\rho_L a^3 \psi_n \sum_{i=0}^{\infty}\sum_{h=0}^{\infty} \tilde{q}_i\tilde{q}_h \sum_{k=0}^{\infty} \frac{(A_{in}\beta_{ink} + C_{in}\gamma_{ink})}{\alpha_{nk}\varepsilon_{nk}} (A_{hn}\beta_{hnk} + C_{hn}\gamma_{hnk}) \tanh\left(\varepsilon_{nk}\frac{H}{a}\right). \tag{35}$$

For axisymmetric modes, equation (30) is replaced by

$$-K_{i00} + \sum_{k=1}^{\infty} K_{i0k}\mathrm{J}_0\left(\varepsilon_{0k}\frac{r}{a}\right)\frac{\varepsilon_{0k}}{a\tanh(\varepsilon_{0k}H/a)} = \left[A_{i0}\mathrm{J}_0\left(\frac{\lambda_{i0}r}{a}\right) + C_{i0}\mathrm{I}_0\left(\frac{\lambda_{i0}r}{a}\right)\right]. \tag{36}$$

The constant K_{i00} is given by

$$\frac{K_{i00}}{2} = -\int_0^1 [A_{i0}\mathrm{J}_0(\lambda_{i0}\rho) + C_{i0}\mathrm{I}_0(\lambda_{i0}\rho)]\rho\,\mathrm{d}\rho = -\tau_{i0}, \tag{37}$$

where [18]

$$\tau_{i0} = [(A_{i0}/\lambda_{i0})\mathrm{J}_1(\lambda_{i0}) + (C_{i0}/\lambda_{i0})\mathrm{I}_1(\lambda_{i0})]. \tag{38}$$

The constants K_{i0k}, for $k > 0$, are obtained by equation (31) computed for $n = 0$; therefore, for axisymmetric modes, the term $T_L^{*(2)}$ of the reference kinetic energy of the liquid is given by

$$T_L^{*(2)} = \tfrac{1}{2}\rho_L a^3 \psi_n \sum_{i=0}^{\infty}\sum_{h=0}^{\infty} \tilde{q}_i\tilde{q}_h \left[2\frac{H}{a}\tau_{i0}\tau_{h0} + \sum_{k=1}^{\infty} \frac{(A_{i0}\beta_{i0k} + C_{i0}\gamma_{i0k})}{\alpha_{0k}\varepsilon_{0k}} \times (A_{h0}\beta_{h0k} + C_{h0}\gamma_{h0k}) \tanh\left(\varepsilon_{0k}\frac{H}{a}\right)\right]. \tag{39}$$

3.4. COUPLING EFFECT OF THE LIQUID

In Section 3.1 it was shown that the reference kinetic energy of the liquid is not given by the simple sum $T_L^{*(1)} + T_L^{*(2)}$, but is given by four terms; this fact can be justified as the coupling effect of the liquid. In fact, even if one eliminates the presence of the coupling spring between the plate and the shell, these two elements result, coupled by the presence of the liquid inside the tank. In particular, the quantity $T_L^{*(1-2)}$, for asymmetric modes, is given by

$$T_L^{*(1-2)} = \tfrac{1}{2}\rho_L \int_{S_1} (\phi^{(2)})_{r=a} w\,\mathrm{d}S$$

$$= \tfrac{1}{2}\rho_L B a^2 \psi_n \sum_{s=1}^{\infty}\sum_{i=0}^{\infty} q_s\tilde{q}_i \sum_{k=0}^{\infty} K_{ink}\mathrm{J}_n(\varepsilon_{nk})\left[\zeta_{snk}^{(1)} - \frac{\zeta_{snk}^{(2)}}{\tanh(\varepsilon_{nk}H/a)}\right], \tag{40}$$

where the constants K_{ink} are given by equation (31) and

$$\zeta_{snk}^{(1)} = \frac{(s\pi a/L) - (s\pi a/L)\cos(s\pi H/L)\cosh(\varepsilon_{nk}H/a) + \varepsilon_{nk}\sin(s\pi H/L)\sinh(\varepsilon_{nk}H/a)}{\varepsilon_{nk}^2 + s^2\pi^2 a^2/L^2}, \tag{41}$$

$$\zeta_{snk}^{(2)} = \frac{-(s\pi a/L)\cos(s\pi H/L)\sinh(\varepsilon_{nk}H/a) + \varepsilon_{nk}\sin(s\pi H/L)\cosh(\varepsilon_{nk}H/a)}{\varepsilon_{nk}^2 + s^2\pi^2 a^2/L^2}, \tag{42}$$

The quantity $T_L^{*(1-2)}$, for axisymmetric modes ($n = 0$), is given by

$$T_L^{*(1-2)} = \tfrac{1}{2}\rho_L B a^2 \psi_n \sum_{s=1}^{\infty}\sum_{i=0}^{\infty} q_s \tilde{q}_i \left\{ K_{i00}\zeta_s^{(0)} + \sum_{k=1}^{\infty} K_{i0k} \mathrm{J}_0(\varepsilon_{0k}) \left[\zeta_{s0k}^{(1)} - \frac{\zeta_{s0k}^{(2)}}{\tanh(\varepsilon_{0k}H/a)} \right] \right\}, \tag{43}$$

where

$$\zeta_s^{(0)} = \frac{-(s\pi a/L)H + a\sin(s\pi H/L)}{(s\pi a/L)^2}. \tag{44}$$

The last component of the reference kinetic energy of the liquid is the term $T_L^{*(2-1)}$ that has the following expression for both axisymmetric and asymmetric modes:

$$T_L^{*(2-1)} = \tfrac{1}{2}\rho_L \int_{S_2} (\phi^{(1)})_{x=0} w_P \, \mathrm{d}S = \tfrac{1}{2}\rho_L B a^2 \psi_n \sum_{s=1}^{\infty}\sum_{i=0}^{\infty} q_s \tilde{q}_i$$

$$\times \sum_{m=1}^{\infty} \left\{ 4\sigma_{ms} \Big/ \left[(2m-1)\pi \mathrm{I}_n'\left(\frac{2m-1}{2}\pi\frac{a}{H} \right) \right] \right\} (A_{in}\xi_{imn}^{(1)} + C_{in}\xi_{imn}^{(2)}), \tag{45}$$

Here, the constants σ_{ms} are given by equations (24a,b) and

$$\xi_{imn}^{(1)} = \frac{\dfrac{2m-1}{2}\pi\dfrac{a}{H}}{\left(\dfrac{2m-1}{2}\pi\dfrac{a}{H} \right)^2 + \lambda_{in}^2} \mathrm{J}_n(\lambda_{in}) \mathrm{I}_n'\left(\frac{2m-1}{2}\pi\frac{a}{H} \right), \tag{46}$$

$$\xi_{imn}^{(2)} = \left[\lambda_{in}\mathrm{I}_n\left(\frac{2m-1}{2}\pi\frac{a}{H} \right)\mathrm{I}_n'(\lambda_{in}) - \frac{2m-1}{2}\pi\frac{a}{H}\mathrm{I}_n(\lambda_{in}) \right.$$

$$\left. \times \mathrm{I}_n'\left(\frac{2m-1}{2}\pi\frac{a}{H} \right) \right] \Big/ \left[\lambda_{in}^2 - \left(\frac{2m-1}{2}\pi\frac{a}{H} \right)^2 \right]. \tag{47}$$

4. THE EIGENVALUE PROBLEM

For the numerical calculation of the natural frequencies and the unknown parameters describing modes, only N terms in the expansion of w, equation (1), and $\tilde{N} + 1$ in the expansion of w_P, equation (4), are considered, where N and $\tilde{N}$ are chosen large enough to give the required accuracy to the solution. Therefore, all of the energies are given by

finite summations. It is convenient to introduce a vectorial notation; the vector $\mathbf{q}$ of the unknown parameters is defined by

$$\mathbf{q} = \begin{Bmatrix} \{q\} \\ \text{- - -} \\ \{\tilde{q}\} \end{Bmatrix}, \tag{48}$$

where

$$\{q\} = \begin{Bmatrix} q_1 \\ \vdots \\ q_N \end{Bmatrix} \quad \text{and} \quad \{\tilde{q}\} = \begin{Bmatrix} \tilde{q}_0 \\ \vdots \\ \tilde{q}_N \end{Bmatrix}. \tag{49}$$

The maximum potential energy of the shell becomes

$$V_S = \tfrac{1}{2}\rho_S h_S a(L/2)\psi_n B^2 \mathbf{q}^{\mathrm{T}} \mathbf{K_S} \mathbf{q}. \tag{50}$$

The partitioned matrix $\mathbf{K_S}$ is

$$\mathbf{K_S} = \left[\begin{array}{c|c} [\boldsymbol{\omega}_1] & [\mathbf{0}] \\ \hline [\mathbf{0}] & [\mathbf{0}] \end{array}\right], \tag{51}$$

where the elements of the diagonal submatrix $[\boldsymbol{\omega}_1]$ are given by

$$\omega_{1_{sj}} = \delta_{sj}\omega_s^2, \qquad s, j = 1, \ldots, N, \tag{52}$$

and δ_{sj} is the Kronecker delta. The maximum potential energy of the plate can be written as

$$V_P = \tfrac{1}{2}(D/a^2)\psi_n \mathbf{q}^{\mathrm{T}} \mathbf{K_P} \mathbf{q}. \tag{53}$$

The matrix $\mathbf{K_P}$ is

$$\mathbf{K_P} = \left[\begin{array}{c|c} [\mathbf{0}] & [\mathbf{0}] \\ \hline [\mathbf{0}] & [\boldsymbol{\lambda}_1] \end{array}\right], \tag{54}$$

where the elements of the diagonal submatrix $[\boldsymbol{\lambda}_1]$ are given by

$$\lambda_{1_{ih}} = \delta_{ih}\lambda_{ih}^4, \qquad i, h = 0, \ldots, \tilde{N}. \tag{55}$$

The maximum potential energy stored by the coupling spring can be written as

$$V_C = \tfrac{1}{2}c_1 a \psi_n \mathbf{q}^{\mathrm{T}} \mathbf{K_C} \mathbf{q}. \tag{56}$$

The matrix $\mathbf{K_C}$ is

$$\mathbf{K_c} = \left[\begin{array}{c|c} [\mathbf{K}_1] & [\mathbf{K}_2] \\ \hline [\mathbf{K}_2]^{\mathrm{T}} & [\mathbf{K}_3] \end{array}\right], \tag{57}$$

where the elements of the submatrices $[\mathbf{K}_i]$ are given in Appendix A. The maximum potential energy stored by the Winkler elastic foundation can be written as

$$V_B = \tfrac{1}{2}k' a^2 \psi_n \mathbf{q}^{\mathrm{T}} \mathbf{K_B} \mathbf{q}. \tag{58}$$

The matrix is $\mathbf{K_B}$ is

$$\mathbf{K_B} = \left[\begin{array}{c|c} [\mathbf{0}] & [\mathbf{0}] \\ \hline [\mathbf{0}] & [\mathbf{I}] \end{array}\right], \tag{59}$$

where [**I**] is the identity $(\tilde{N}+1)\times(\tilde{N}+1)$ submatrix. The reference kinetic energy of the shell, equation (7), can be written as

$$T_S^* = \tfrac{1}{2}\rho_S h_S a(L/2)\psi_n B^2 \mathbf{q}^{\mathrm{T}}\mathbf{M_S}\mathbf{q}. \tag{60}$$

The matrix $\mathbf{M_S}$ is

$$\mathbf{M_S} = \left[\begin{array}{c|c} [\mathbf{I}] & [\mathbf{0}] \\ \hline [\mathbf{0}] & [\mathbf{0}] \end{array}\right], \tag{61}$$

where [**I**] is the $N \times N$ identity matrix. The reference kinetic energy of the plate, equation (8), can be written as

$$T_P^* = \tfrac{1}{2}\rho_P h_P a^2 \psi_n \mathbf{q}^{\mathrm{T}}\mathbf{M_P}\mathbf{q}, \tag{62}$$

The matrix $\mathbf{M}_P$ is

$$\mathbf{M_P} = \left[\begin{array}{c|c} [\mathbf{0}] & [\mathbf{0}] \\ \hline [\mathbf{0}] & [\mathbf{I}] \end{array}\right], \tag{63}$$

where [**I**] is the identity $(\tilde{N}+1)\times(\tilde{N}+1)$ submatrix. The reference kinetic energy of the liquid can be written as

$$T_L^* = \tfrac{1}{2}\rho_L a\psi_n \mathbf{q}^{\mathrm{T}}\mathbf{M_L}\mathbf{q}, \tag{64}$$

where $\mathbf{M_L}$ is a symmetric partitioned matrix of dimension $(N+(\tilde{N}+1))\times(N+(\tilde{N}+1))$:

$$\mathbf{M_L} = \left[\begin{array}{c|c} [\mathbf{M}_1] & [\mathbf{M}_2] \\ \hline [\mathbf{M}_2]^T & [\mathbf{M}_3] \end{array}\right], \tag{65}$$

where the elements of the submatrices $[\mathbf{M}_i]$ are given in Appendix B. Hence it is useful to introduce the Rayleigh quotient for coupled fluid-structure vibrations [33]. The Rayleigh quotient can be written as

$$(V_S + V_P + V_C + V_B)/(T_S^* + T_P^* + T_L^*). \tag{66}$$

Thus, the values of the vector $\mathbf{q}$ of the unknown parameters are determined in order to render equation (66) stationary [15], and the following Galerkin equation is obtained:

$$\begin{aligned}(\tfrac{1}{2}B^2\rho_S h_S a L\mathbf{K_s} + (D/a^2)\mathbf{K_P} + c_1 a\mathbf{K_C} + k_1 a^2\mathbf{K_B})\mathbf{q} \\ - \Lambda^2(\tfrac{1}{2}B^2\rho_S h_S a L\mathbf{M_s} + \rho_P h_P a^2\mathbf{M_P} + \rho_L a\mathbf{M_L})\mathbf{q} = 0,\end{aligned} \tag{67}$$

where Λ is the circular frequency (rad/s) of the tank partially filled with liquid. Equation (67) gives a linear eigenvalue problem for a real, symmetric matrix.

TABLE 1

The circular frequencies ω (rad/s) *of the plate-ended circular cylindrical shell studied in reference* [6]; *only modes having* $n = 4$ *circumferential waves are considered*; *the results obtained by using the approach presented are compared to the data given by Huang and Soedel* [6]

Mode	Present study	Huang and Soedel [6]	Difference (%)
First	8 520·94	8 518	0·03
Second	19 885·6	19 650	1·2
Third	21 466·5	21 031	2·0
Fourth	31 656·8	31 640	0·05
Fifth	39 407·3	39 328	0·2
Sixth	42 299·1	41 509	1·9

5. NUMERICAL RESULTS

5.1. COMPARISON WITH AVAILABLE RESULTS

The numerical solution to the eigenvalue problem, equation (67), is obtained by using the *Mathematica* [34] computer program. Ten shell modes and ten plate modes are considered in the Rayleigh–Ritz expansion. To check the theory used, the numerical results obtained by using the present approach were compared to the data presented by Huang and Soedel [6] for an empty plate-ended circular cylindrical shell. The plate and the shell are assumed to be joined by a spring of infinite stiffness c_1. For infinity, one in fact takes a large enough quantity in the calculations. In practice, one sometimes considers a trial value of the spring stiffness and then changes it until one obtains eigenvalues that are not affected by an increment in the stiffness value. However, one can give directly a stiffness value much larger than the plate and shell edge stiffness. Both the shell and the plate considered in reference [6] are made of a steel with the following material properties: $E = 206$ GPa, $\rho_S = \rho_P = 7850\ \mathrm{Kg\,m^{-3}}$ and $\nu = 0{\cdot}3$. The dimensions are: $a = 0{\cdot}1$ m, $L = 0{\cdot}2$ m and $h_S = h_P = 2$ mm. The comparison is shown in Table 1 for modes having $n = 4$ nodal diameters. A very good agreement between the natural frequencies given in reference [6], obtained by using the receptance method, and the present results was found. Obviously, this test does not validate the liquid–tank interaction theory studied in section 3.

TABLE 2

The circular frequencies ω (rad/s) *of the circular cylindrical shell studied in references* [23, 25]; *only axisymmetric bulging modes* ($n = 0$) *are considered*; *the results obtained by using the approach presented are compared to the data given by Kondo* [23] *and Gupta and Hutchinson* [25]

Mode	Present study	Kondo exact solution [23]	Kondo series solution [23]	Gupta and Hutchinson [25]
First	22·23	22·09557	22·33470	22·3494
Second	44·00	43·76193	44·12022	44·1699
Third	57·19	56·82922	57·21935	58·2442
Fourth	67·29	66·88753	67·30628	69·5125
Fifth	75·84	75·34688	75·85164	79·1894

TABLE 3

The natural frequencies (Hz) *of the circular bottom plate studied in reference* [32]; *only axisymmetric bulging modes* ($n = 0$) *are considered*; *the results obtained by using the approach presented are compared to the data given by Chiba* [32] *for two different water levels*: $H/a = 0{\cdot}2,\ 1$

	$H/a = 0{\cdot}2$		$H/a = 1$	
Mode	Present study	Chiba [32]	Present study	Chiba [32]
First	148	144	100	97
Second	617	614	520	515
Third	1505	1510	1397	1406

Circular frequencies (rad/s) obtained by using the proposed method are compared in Table 2 with results obtained by Kondo [23] and Gupta and Hutchinson [25] for the axisymmetric bulging modes ($n = 0$) of a circular cylindrical shell simply supported at both ends ($c_1 = 0$) and having the following dimensions: $a = 25$ m, $L = 30$ m, $H = 21{\cdot}6$ m and $h_S = 0{\cdot}03$ m. The shell is considered made of a steel with the following material properties: $E = 206$ GPa, $\rho_S = 7850$ Kg m^{-3} and $v = 0{\cdot}3$; the base of the tank is rigid and the liquid inside the shell is water, having $\rho_L = 1000$ kg m^{-3}. The results obtained are compared to the data given in reference [23] and obtained by using both the exact solution and the Fourier series solution, and to results given in reference [25] and obtained by an approximate formula. It is clear that the present results are closer to the exact solution than the Fourier series results [23] and the approximate results of reference [25].

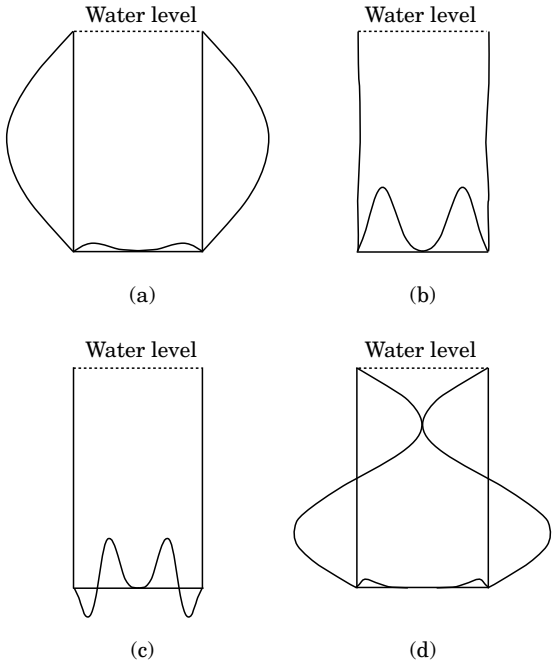

Figure 2. The first four mode shapes with $n = 4$ nodal diameters of the tank having $h_P = 0{\cdot}55$ mm and $H = 0{\cdot}6$ m. Natural frequencies: (a) 100·86 Hz; (b) 124·49 Hz; (c) 292·08 Hz; (d) 319·66 Hz.

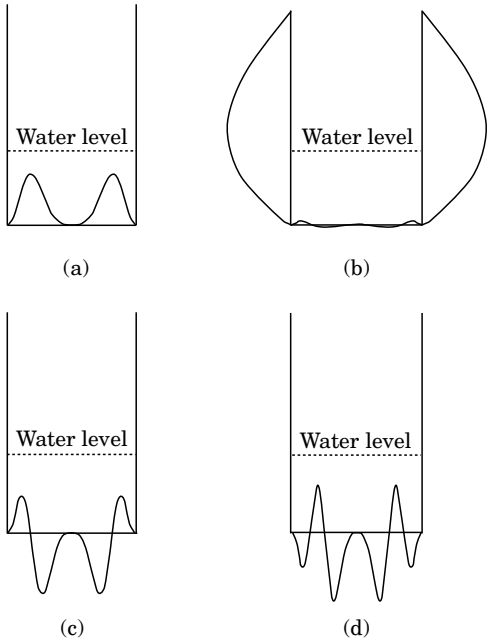

Figure 3. The first four mode shapes with $n = 4$ nodal diameters of the tank having $h_P = 0{\cdot}55$ mm and $H = 0{\cdot}2$ m. Natural frequencies: (a) 124·47 Hz; (b) 187·48 Hz; (c) 292·05 Hz; (d) 536·84 Hz.

A further comparison is then also given in order to check the theory proposed to investigate the liquid–plate coupled vibrations. To this aim, the results given by Chiba [32] for a circular bottom plate clamped to a rigid circular cylindrical shell are compared with the results of the proposed theory for two different levels of water inside the tank. The plate dimensions are: $a = 0{\cdot}144$ m and $h_P = 2$ mm, and the plate's material is a steel having $E = 206$ GPa, $\rho_P = 7850$ kg m^{-3} and $\nu = 0{\cdot}25$ [32]. The natural frequencies (Hz) of axisymmetric bulging modes ($n = 0$) are compared in Table 3 and a good agreement is verified; it is to be noted that the data in reference [32] are given in diagrammatic form, so that the actual values could be little different from those reported in Table 3. It is interesting to observe that the conditions of rigid shell or rigid bottom plate can be obtained by the proposed theory, giving a very high value to the Young's modulus of the corresponding element ($E \to \infty$).

5.2. NEW RESULTS FOR TALL AND SHALLOW TANKS

The study is now addressed to tanks partially filled with water, having $\rho_L = 1000$ kg m^{-3}. In the cases studied, both the shell and the plate are assumed to be made of steel with the following material properties: $E = 206$ GPa, $\rho_S = \rho_P = 7800$ kg m^{-3} and $\nu = 0{\cdot}3$ (the mass density of this steel is little different from that considered in section 5.1). Tall tanks ($L \geqslant 2a$) are initially considered; the dimensions fixed for all computations relative to this case are: $a = 0{\cdot}175$ m, $L = 0{\cdot}6$ m and $h_S = 1$ mm. The elastic foundation is initially not considered ($k_1 = 0$), and the plate and the shell are considered to be coupled by a spring with infinite (in practice) stiffness at the joint ($c_1 \to \infty$).

First, a tank with a bottom plate having a thickness $h_P = 0{\cdot}55$ mm and being completely water-filled ($H = 0{\cdot}6$ m) is studied. The first four mode shapes having $n = 4$ nodal diameters are given in Figure 2. Mode shapes are plotted in the tank cross-section defined by $\theta = 0$ and $\theta = \pi$. The mode shapes with an even number n of nodal diameters

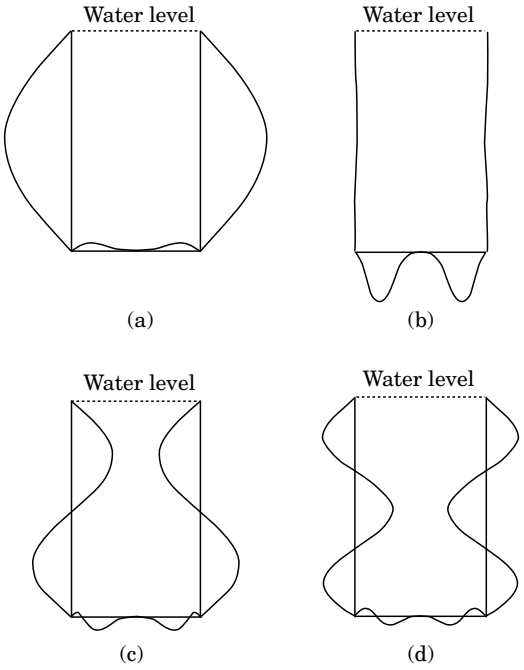

Figure 4. The first four mode shapes with $n = 4$ nodal diameters of the tank having $h_P = 1$ mm and $H = 0{\cdot}6$ m. Natural frequencies: (a) 101·08 Hz; (b) 287·96 Hz; (c) 320·28 Hz; (d) 607·81 Hz.

are symmetric with respect to the longitudinal axis, whereas those modes with an odd number n are antisymmetric. In Figure 2 there are symmetric mode shapes; the first (Figure 2(a)) and fourth (Figure 2(d)) modes are shell-dominant (shell displacement larger than plate displacement), while the second (Figure 2(b)) and third (Figure 2(c)) are plate-dominant. It is clear that, due to the relatively small plate thickness, the plate is dragged by the shell. If one neglects the coupling effect of the liquid ($T_L^{*(1-2)} = T_L^{*(2-1)} = 0$) in the computation of the natural frequencies one obtains the following results: first mode

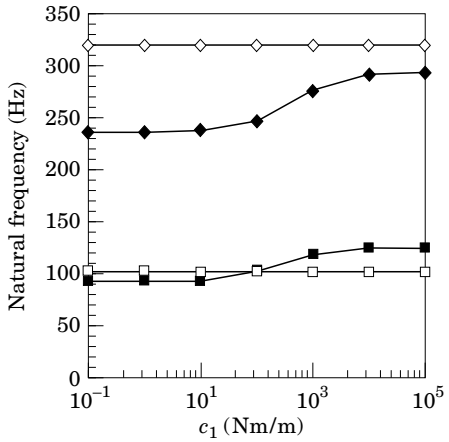

Figure 5. The effect of the spring stiffness c_1 on the natural frequencies (Hz) of the first four modes, with four nodal diameters, of the tank having $h_P = 0{\cdot}55$ mm and $H = 0{\cdot}6$ m. The first two plate-dominant modes and the first two shell-dominant modes are given. ——■——, P1; ——◆——, P2; ——□——, S1; ——◇——. S1.

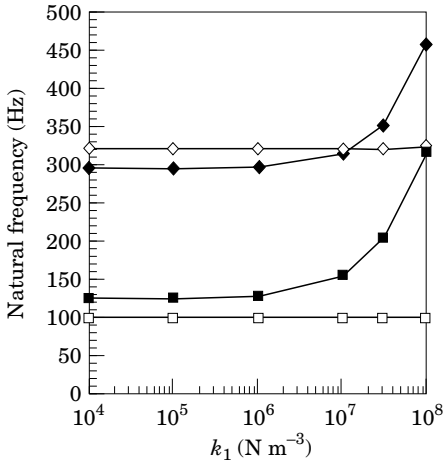

Figure 6. The effect of the elastic Winkler foundation stiffness k_1 on the natural frequencies of the first four modes, with four nodal diameters, of the tank having $h_P = 0{\cdot}55$ mm, $H = 0{\cdot}6$ m and $c_1 = \infty$. The first two plate-dominant modes and the first two shell-dominant modes are given. Key as Figure 5.

100·79 Hz, second mode 124·49 Hz, third mode 291·64 Hz and fourth mode 319·72 Hz. These results are close to the actual frequencies given in the caption of Figure 2. Therefore the coupling effect of the liquid is not great in this case.

In Figure 3, the same tank is considered to be partially filled with a level of water $H = 0{\cdot}2$ m and modes with $n = 4$ are considered. The natural frequencies are obviously higher than in the preceding case and the mode shapes are changed. In this case, the first and second modes are shell-dominant and the third and fourth are plate-dominant.

In Figure 4 the tank with the bottom plate of thickness $h_P = h_S = 1$ mm is considered to be completely water-filled ($H = 0{\cdot}6$ m and $n = 4$). The plate has now a greater flexural stiffness than in the two preceding cases. In fact, upon comparing Figures 2(a) and 4(a), it is clear that the plate is now less dragged by the shell. Moreover, the natural frequencies

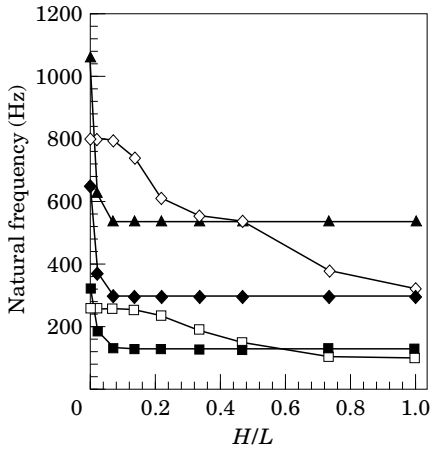

Figure 7. Natural frequencies as functions of the depth ratio H/L. Modes with four nodal diameters of the tank with $h_P = 0{\cdot}55$ mm. The first three plate-dominant modes (P1, P2 and P3) and the first two shell-dominant modes (S1 and S2) are reported. Key as Figure 5, with ——▲——, P3.

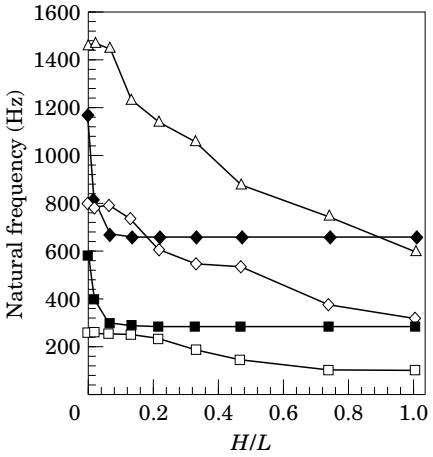

Figure 8. Natural frequencies as functions of the depth ratio H/L. Modes with four nodal diameters of the tank with $h_P = 1$ mm. The first two plate-dominant modes (P1 and P2) and the first three shell-dominant modes (S1, S2 and S3) are reported. Key as Figure 5, with ——△——, S3.

of the shell-dominant modes are less affected by the increase of the plate thickness than plate-dominant modes.

The effect of the spring stiffness c_1 at the shell–plate joint is illustrated in Figure 5 for the completely water-filled tank with $h_P = 0{\cdot}55$ mm and $n = 4$. This figure shows that some modes are more sensitive to the spring stiffness than others and that a stiffness $c_1 = 10^6$ [Nm/m] can be used to simulate an infinite stiffness in computations, for the tank considered. It is also interesting to remember that, due to the artificial spring method used, all the axisymmetric conditions at the plate–shell joint can be simulated by changing only the spring stiffness value c_1.

The presence of an elastic Winkler foundation is now considered for the same tank completely water-filled with $n = 4$ and $c_1 \to \infty$. It is interesting to note that in Figure 6, due to the low relatively flexural stiffness of the plate considered, the first mode is little affected

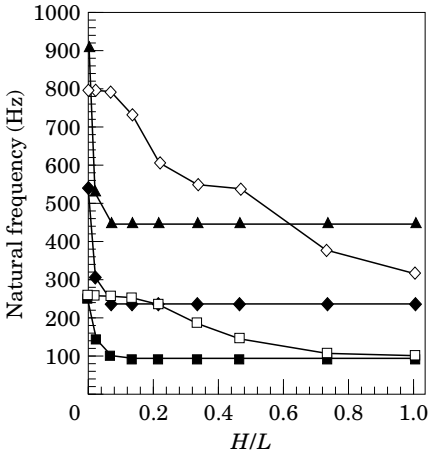

Figure 9. Natural frequencies as functions of the depth ratio H/L; the plate and the shell are both considered to be uncoupled. Modes with four nodal diameters of the plate with $h_P = 0{\cdot}55$ mm. The first three plate modes (P1, P2 and P3) and the first two shell modes (S1 and S2) are reported. Key as Figure 7.

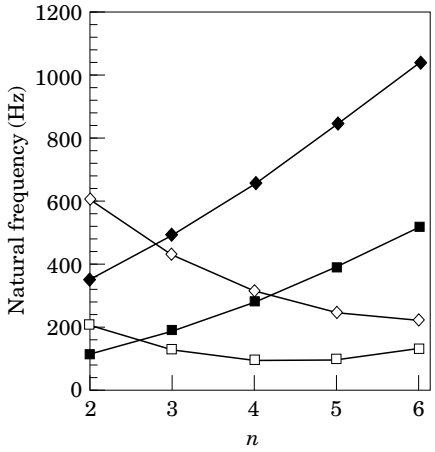

Figure 10. Natural frequencies as functions of the number of nodal diameters n: modes of the completely water-filled tank with $h_P = 1$ mm. The first two plate-dominant modes (P1 and P2) and the first two shell-dominant modes (S1 and S2) are given. Key as Figure 5.

by the increase of the foundation stiffness k_1. On the contrary, plate-dominant modes are greatly affected by a change of k_1.

The natural frequencies of the tank as function of the depth ratio H/L are shown in Figures 7 and 8 for two different values of the thickness h_P of the bottom plate and for $n = 4$. Plate-dominant modes show similar curves, that are different from curves relative to shell-dominant modes. Figure 9 is similar to Figures 7 and 8, but it relates to the shell and the plate vibrating completely uncoupled, considering the other component of the tank to be rigid; so that there is no coupling effect due to the spring and to the liquid. A comparison of Figures 7 and 9, that are relative to the tank having $h_P = 0{\cdot}55$ mm, shows that the natural frequencies of plate-dominant modes decrease in the uncoupled case, Figure 9; for shell-dominant modes this phenomenon is almost

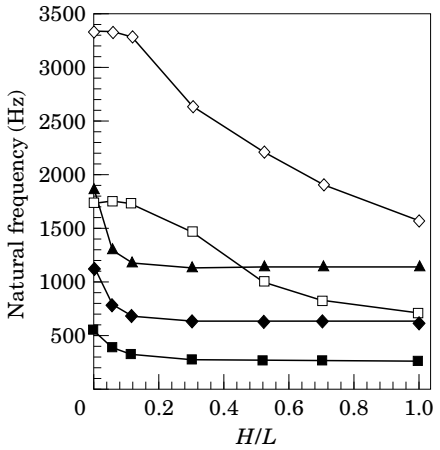

Figure 11. Natural frequencies as functions of the depth ratio H/L for the shallow tank studied. The first three plate-dominant modes (P1, P2 and P3) and the first two shell-dominant modes (S1 and S2) with four nodal diameters are considered. Key as Figure 7.

imperceptible, due to the low flexural stiffness of the plate considered with respect to shell flexural stiffness.

The natural frequencies as functions of the number of nodal diameters n are given in Figure 10 for the completely water-filled tank with 1 mm plate thickness. For the tank considered, the shell-dominant mode having the lower frequency has $n = 4$ nodal diameters, whereas the plate-dominant mode having the lower frequency has no nodal diameters ($n = 0$); obviously, the first shell-dominant mode has no nodal circles (excluding at the edges), as well as the first plate-dominant mode.

The results given so far refer to tall tanks whereas natural frequencies (Hz) relating to a shallow tank are reported in Figure 11. The tank dimensions are: $a = L = 0{\cdot}175$ m, $h_S = h_P = 1$ mm and $H = 0 \div 0{\cdot}175$ m. Also, for this shallow tank one can see that the effect of the liquid plays an important role on the natural frequencies.

6. CONCLUSIONS

The vibration problem of circular cylindrical tanks, partially filled with liquids has a relevant role in many engineering applications. The artificial spring method allows a flexible and accurate description of the system; the inclusion of other complicating effects, not considered in the present paper, is made possible by using the same procedure. This approach, already successfully used in the study of the empty plate-ended circular cylindrical shell and its internal sound field, can be used to describe the free vibrations of the fluid-loaded structure. If one is interested only in bulging modes, a zero dynamic pressure can be imposed on the free liquid surface, neglecting the free surface waves, and the solution of the coupled liquid–structure problem is obtained by a linear eigenvalue problem.

It was found that the natural frequencies and mode shapes of thin walled tanks are greatly affected by the presence of different water levels inside. An interesting shell–plate coupling is observed in mode shapes; this coupling is due both to the artificial spring, which simulates the shell–plate joint, and to the liquid inside the tank. The presence of a joint that can be modelled with opportune stiffness in order to simulate the actual behaviour of the shell–plate system and the effect considered of an elastic Winkler foundation also makes the model more realistic for some engineering applications.

REFERENCES

1. J. Yuan and S. M. Dickinson 1992 *Journal of Sound and Vibration* **152**, 203–216. On the use of artificial springs in the study of the free vibrations of systems comprised of straight and curved beams.
2. L. Cheng and J. Nicolas 1992 *Journal of Sound and Vibration* **155**, 231–247. Free vibration analysis of a cylindrical shell–circular plate system with general coupling and various boundary conditions.
3. J. Yuan and S. M. Dickinson 1992 *Journal of Sound and Vibration* **159**, 39–55. The flexural vibration of rectangular plate systems approached by using artificial springs in the Rayleigh–Ritz method.
4. J. Yuan and S. M. Dickinson 1994 *Journal of Sound and Vibration* **175**, 241–263. The free vibration of circularly cylindrical shell and plate systems.
5. G. Yamada, T. Irie, and T. Tamiya 1986 *Journal of Sound and Vibration* **108**, 297–304. Free vibration of a circular cylindrical double-shell system closed by end plates.
6. D. T. Huang and W. Soedel 1993 *Journal of Sound and Vibration* **162**, 403–427. Natural frequencies and modes of a circular plate welded to a circular cylindrical shell at arbitrary axial positions.

7. D. T. Huang and W. Soedel 1993 *Journal of Sound and Vibration* **166**, 315–339. On the free vibrations of multiple plates welded to a cylindrical shell with special attention to mode pairs.
8. D. T. Huang and W. Soedel 1993 *Journal of Sound and Vibration* **166**, 341–369. Study of the forced vibration of shell-plate combinations using the receptance method.
9. L. Cheng 1994 *Journal of Sound and Vibration* **174**, 641–654. Fluid–structural coupling of a plate-ended cylindrical shell: vibration and internal sound field.
10. H. F. Bauer and J. Siekmann 1971 *Ingenieur Archiv* **40**, 266–280. Dynamic interaction of a liquid with the elastic structure of a circular cylindrical container.
11. A. W. Leissa 1973 *Vibration of Shells*. *NASA SP*-288. Washington, D.C.: U.S. Government Printing Office.
12. M. Chiba 1994 *Journal of Sound and Vibration* **169**, 387–394. Axisymmetric free hydroelastic vibration of a flexural bottom plate in a cylindrical tank supported on an elastic foundation.
13. A. W. Leissa 1969 *Vibration of Plates*. *NASA SP*-160. Washington, DC: Government Printing Office.
14. L. L. Faulkner 1969 *Ph.D. Thesis*, *Purdue University*. Vibration analysis of shell structures using receptances.
15. L. Meirovitch 1986 *Elements of Vibration Analysis*. New York: McGraw-Hill; (second edition). See pp. 270–282.
16. M. Amabili, G. Frosali and M. K. Kwak 1996 *Journal of Sound and Vibration* **191**, 825–846. Free vibrations of annular plates coupled with fluids.
17. A. W. Leissa and Y. Narita 1980 *Journal of Sound and Vibration* **70**, 221–229. Natural frequencies of simply supported circular plates.
18. A. D. Wheelon 1968 *Tables of Summable Series and Integrals Involving Bessel Functions*. San Francisco: Holden-Day.
19. H. J.-P. Morand and R. Ohayon 1992 *Interactions Fluides–Structures*. Paris: Masson. See pp. 71–72. (English edition: 1995 *Fluid Structure Interaction*. New York: John Wiley)
20. H. Lamb 1945 *Hydrodynamics*. New York: Dover. See p. 46.
21. J. G. Berry and E. Reissner 1958 *Journal of Aeronautical Science* **25**, 288–294. The effect of an internal compressible fluid column on the breathing vibrations of a thin pressurized cylindrical shell.
22. U. S. Lindholm, D. D. Kana and H. N. Abramson 1962 *Journal of Aeronautical Science* **29**, 1052–1059. Breathing vibrations of a circular cylindrical shell with an internal liquid.
23. H. Kondo 1981 *Bulletin of the Japan Society of Mechanical Engineers* (*JSME*) **24**, 215–221. Axisymmetric vibration analysis of a circular cylindrical tank.
24. N. Yamaki, J. Tani and T. Yamaji 1984 *Journal of Sound and Vibration* **94**, 531–550. Free vibration of a clamped–clamped circular cylindrical shell partially filled with liquid.
25. R. K. Gupta and G. L. Hutchinson 1988 *Journal of Sound and Vibration* **122**, 491–506. Free vibration analysis of liquid storage tanks.
26. M. Amabili and G. Dalpiaz 1995 *Transactions of the American Society of Mechanical Engineers*, *Journal of Vibration and Acoustics* **117**, 187–191. Breathing vibrations of a horizontal circular cylindrical tank shell, partially filled with liquid.
27. M. Amabili 1996 *Journal of Sound and Vibration* **191**, 757–780. Free vibration of partially filled, horizontal cylindrical shells.
28. M. Amabili and G. Dalpiaz 1995 *Proceedings of the International Forum on Aeroelasticity and Structural Dynamics*, 26–28 *June*, *Manchester*, *U.K.* **1**, 38.1–38.8. Vibration of a fluid-filled circular cylindrical tank: axisymmetric modes of the elastic bottom plate.
29. M. Amabili *Shock and Vibration* (to appear). Bulging modes of circular bottom plates in rigid cylindrical containers filled with a liquid.
30. G. Bhuta and L. R. Koval 1964 *Journal of the Acoustical Society of America* **36**, 2071–2079. Hydroelastic solution of the sloshing of a liquid in a cylindrical tank.
31. M. Chiba 1992 *Journal of Fluids and Structures* **6**, 181–206. Nonlinear hydroelastic vibration of a cylindrical tank with an elastic bottom, containing liquid, part I: experiment.
32. M. Chiba 1993 *Journal of Fluids and Structures* **7**, 57–73. Nonlinear hydroelastic vibration of a cylindrical tank with an elastic bottom, containing liquid, part II: linear axisymmetric vibration analysis.
33. F. Zhu 1994 *Journal of Sound and Vibration* **171**, 641–649. Rayleigh quotients for coupled free vibrations.
34. S. Wolfram 1991 *Mathematica*: *a System for Doing Mathematics by Computer*. Redwood, CA: Addison Wesley; second edition.

APPENDIX A: SPRING MATRIX $\mathbf{K}_C$

In this appendix, the partitioned spring matrix $\mathbf{K}_C$, equation (57), is reported. The elements of the spring submatrix $\mathbf{K}_1$ of dimension $N \times N$ are given by

$$(K_1)_{sj} = B^2(\pi^2/L^2)sj. \tag{A1}$$

The elements of the spring submatrix $\mathbf{K}_2$ of dimension $N \times (\tilde{N}+1)$ are given by

$$(K_2)_{si} = -B(\pi/L)s(\lambda_{in}/a)[A_{in}\mathrm{J}'_n(\lambda_{in}) + C_{in}\mathrm{I}'_n(\lambda_{in})]. \tag{A2}$$

The elements of the spring submatrix $\mathbf{K}_3$ of dimension $(\tilde{N}+1) \times (\tilde{N}+1)$ are given by

$$(K_3)_{ih} = (\lambda_{in}/a)(\lambda_{hn}/a)[A_{in}\mathrm{J}'_n(\lambda_{in}) + C_{in}\mathrm{I}'_n(\lambda_{in})][A_{hn}\mathrm{J}'_n(\lambda_{hn}) + C_{hn}\mathrm{I}'_n(\lambda_{hn})]. \tag{A3}$$

APPENDIX B: MATRIX $\mathbf{M}_L$ FOR PARTIALLY FILLED TANKS

In this appendix, the elements of the partitioned matrix $\mathbf{M}_L$, describing the inertial effect of the liquid inside the tank, are given only for asymmetric modes; the axisymmetric case is easily obtained by using the equations given in section 3. The elements of the submatrix $\mathbf{M}_1$ of dimension $N \times N$ are given by

$$(M_1)_{sj} = B^2 \sum_{m=1}^{\infty} \frac{4\sigma_{ms}\sigma_{jm}}{(2m-1)\pi} \left[\mathrm{I}_n\left(\frac{2m-1}{2}\,\pi\,\frac{a}{H}\right)\right] \Big/ \left[\mathrm{I}_n\left(\frac{2m-1}{2}\,\pi\,\frac{a}{H}\right)\right], \tag{B1}$$

where σ_{ms} are defined in equations (24a,b). The elements of the submatrix $\mathbf{M}_2$ of dimension $N \times (\tilde{N}+1)$ are given by

$$(M_2)_{si} = \tfrac{1}{2}Ba\left\{\sum_{k=0}^{\infty} K_{ink}\mathrm{J}_n(\epsilon_{nk})\left[\zeta^{(1)}_{snk} - \frac{\zeta^{(2)}_{snk}}{\tanh(\epsilon_{nk}H/a)}\right)\right.$$

$$\left. + \sum_{m=1}^{\infty}\left[4\sigma_{ms}\Big/\left[(2m-1)\pi\mathrm{I}'_n\left(\frac{2m-1}{2}\,\pi\,\frac{a}{H}\right)\right]\right](A_{in}\xi^{(1)}_{imn} + C_{in}\xi^{(2)}_{imn})\right\} \tag{B2}$$

where K_{ink}, $\zeta^{(1)}_{snk}$, $\zeta^{(2)}_{snk}$, $\xi^{(1)}_{imn}$, and $\xi^{(2)}_{imn}$ are defined in equations (31), (41), (42), (46) and (47), respectively. The elements of the submatrix $\mathbf{M}_3$ of dimension $(\tilde{N}+1) \times (\tilde{N}+1)$ are given by

$$(M_3)_{ih} = a^2 \sum_{k=0}^{\infty} \frac{(A_{in}\beta_{ink} + C_{in}\gamma_{ink})}{\alpha_{nk}\varepsilon_{nk}}(A_{hn}\beta_{hnk} + C_{hn}\gamma_{hnk}) \tanh\left(\varepsilon_{nk}\,\frac{H}{a}\right). \tag{B3}$$